NOTICE CONCERNING COPYRIGHT RESTRICTIONS

REFERENCES

Jeffers, P.M., Ward, L.M., Woytowitch, L.M., and Wolfe, N.L., 1989. Homogeneous hydrolysis rate constants for selected chlorinated methanes, ethanes, ethenes, and propanes. Environmental Sci. & Technol., v. 23, p. 965–969.

Mabey, W., and Mill, T., 1978. Critical review of hydrolysis of organic compounds in water under environmental conditions. J. Phys. & Chem. Ref. Data, v. 7, no. 2, p. 383–415.

McNab, W.W., and Narasimhan, T.N., 1992. Groundwater geochemistry and VOC degradation patterns at Lawrence Livermore National Laboratory. Lawrence Berkeley Laboratory Report LBL-32586, 47 p.

Mercer, J.W., Skipp, D.C., and Giffin, D., 1990. Basics of pump-and-treat ground-water remediation technology. U.S. Environmental Protection Agency Report 600/8-90/003, 31 p.

Vogel, T.M., Criddle, C.S., and McCarty, P.L., 1987. Transformation of halogenated aliphatic compounds. Environmental Sci. & Technol., v. 21, no. 8, p. 722–736.

6825

Multiple-Peak Response to Tracer Injection Tests in Single Fractures: A Numerical Study

L. Moreno* and C.F. Tsang

In experimental tracer tests carried out in a single fracture zone in crystalline rock, the breakthrough curves obtained using pulse tracer injection have multiple peaks in some situations (Steffen and Steiger, 1988; J. Hadermann, Paul Scherrer Inst., Switzerland, private communication, 1989; Hoehn et al., 1989). In some cases, it is observed that the shape of these breakthrough curves changes when the injection flow rate is varied. Moreover, the behavior of these multi-peaked curves is observed only for a limited range of injection flow rates.

This article presents some recent simulations of tracer tests in a single fracture with variable apertures. The aim of the work is to study the conditions under which the breakthrough curve may present multiple peaks and to determine how the injection flow rate modifies the shape of the curves in different situations. Although the study focuses on multiple peaks observed during tracer tests with pulse injection, the results can be applied to the case of continuous injection. The breakthrough curve for the latter case would show multiple steps, where each step corresponds to the arrival of a pulse in the pulse test.

DESCRIPTION OF THE MODEL

The apertures of a fracture are not constant in magnitude but vary spatially in the fracture plane. Fluid flowing through the fracture seeks out the least resistive pathways. The main flow is expected to occur through a few channels in the fracture plane (Abelin et al., 1985; Neretnieks, 1987). In defining channels, we mean preferred flow paths in the fracture. If the direction of the pressure gradient is changed, then a new pattern of channel networks would emerge, depending on pressure gradients. Tsang and Tsang (1989) demonstrated that they can be characterized stochastically by the same set of parameters as long as the anisotropy of the spatial correlation of the apertures remains relatively small.

Let us assume that we have a fracture with an overall flow under a "regional" pressure gradient. A solution containing the solute is then injected with a given flow rate at a point in the fracture plane. The injection pressure increases the local pressure profile and hence modifies the original flow pattern around the injection point. For a given distribution of the variable apertures, the injection feeds the solute into flow paths that are in the neighborhood of the injection point. The larger the injection flow, the larger the local pressure profile and the larger the number of paths that may be reached by the solute. However, the pattern of these flow paths depends strongly on the variable apertures near the injection point.

More specifically, the spatial distribution of fracture apertures is obtained by using a grid to partition the fracture and assigning a different aperture to each node enclosed by grid lines. The aperture values used are defined by an aperture density distribution (mean aperture $b = 80\ \mu m$ and spread $\sigma_{inb} = 0.5$) and a spatial correlation length (λ/L). A lognormal distribution for these apertures and an exponential fraction for the spatial covariance of the apertures were chosen. Details may be found in Moreno et al. (1988). For the

---

*Department of Chemical Engineering, Royal Institute of Technology, S-100 44 Stockholm, Sweden.

present study the grid is 40 × 40 nodes. An example of the generated variable-aperture fracture is shown in Figure 1.

Now let us locate a production well with pumping flow rate Q at the upper-right corner of the square shown in Figure 1. We may assume that this represents a quarter of the fracture plane with a production well at its center. Then, by symmetry, the upper and right boundaries are closed boundaries and left and lower boundaries are constant-pressure boundaries. The model is an approximation of a case of convergent tracer test in a fracture where the production well may be a drift in which tracer is collected, such as the MI experiment carried out at Grimsel, Switzerland (Hoehn et al., 1989). The location of a tracer injection well, with injection rate q, may be chosen at different points in the fracture plane; and in Figure 1, it is defined by the index (n_x, n_y) of the respective node, where n_x and n_y are between 1 and 40. Typically, q is much less than Q. Fluid flow is then calculated on the assumption that it is proportional to the cube of the aperture at each node. We assumed the apertures to be much smaller than the flow distance in the nodes, so that the influence on pressure drop by the diverging or converging parts of the flow path is negligible. The pressure at each node is calculated from the fluid balance in each node.

The solute transport is simulated using a particle-tracking technique (Schwartz et al., 1983; Robinson, 1984;
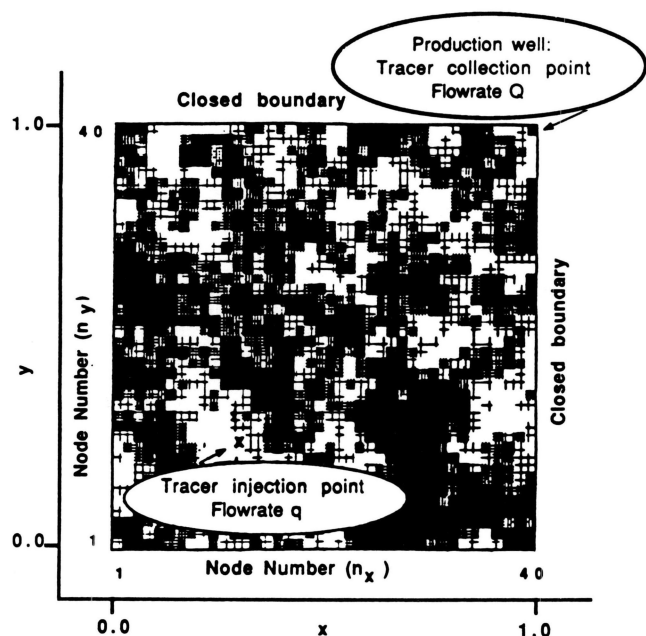
Moreno et al., 1988, 1990). Six thousand particles are introduced in the flow field at the injection node. Each particle is then followed along its path from the injection point to the collection point through the intersections. The particle-tracking method used considers no mixing at these intersections. However, within each branch between adjacent intersections, perfect mixing is assumed (see Moreno et al., 1990). Note that the method includes an intrinsic transverse dispersivity equal to grid size due to numerical dispersion. The residence time of an individual particle over the whole path in the fracture plane is determined as the sum of residence times in all the steps that the particle has traversed. The residence time distribution is then obtained from the residence times of a multitude of individual particle runs.

RESULTS OF THE SIMULATIONS

Flow and solute transport for these different fractures were calculated using the same fracture aperture probability density function and spatial correlation length. Thus they are actually different realizations of the same statistical input parameters. With the production well (see Figure 1) maintained a flow rate Q, tracer injection in a single fracture is simulated for different injection locations and flow rates. For each case, flow paths, solute paths, and breakthrough curves are calculated and plotted. The injection flow rate q is first varied over a wide range (0 to 3% of Q) to determine the interval within which the shape of the breakthrough curves is sensitive to this value. When this interval is found, additional calculations are performed using flow rates within this interval to study in detail the breakthrough curves as a function of flow rates.

In preliminary simulations, we also studied the tracer breakthrough curves as a composite of several partial breakthrough curves, each of which is due to transport of tracer particles through different specified areas in the fracture plane between the injection and collection points. We have computed a number of such partial breakthrough curves. In most cases, when the total breakthrough curve is observed to possess multiple peaks at the collection hole, the partial curves are also found to display multiple peaks. We also noticed that the shape of the curves is predominantly influenced by the condition around the injection point.

The characteristics of the area around the injection point that require further investigation would be (1) the nearby fracture apertures, (2) the existence (or nonexistence) of paths with a large flow rate close to the injection point, and (3) the pressure distribution around the injection point. Large fracture apertures around the injection point may imply large residence times at this location. Conversely, small apertures may cause the injected tracer to be dispersed round the injection point. The existence of paths of large flow close to the injection point would permit a

Figure 1. One realization of variable-aperture fracture. A typical tracer injection point (with injection flow rate q) is marked by "x." The top and right hand-side boundaries are closed, and the bottom and left hand-side boundaries are maintained at a constant pressure relative to the production well. [XBL 935-780]

greater proportion of the tracer flow into these paths. On the other hand, if there are no paths of large flow close to the injection point, the solute has to seek some small and slow paths to flow to the collection hole. The travel times may then be very different from each other, resulting in multiple peaks on the breakthrough curves. The pressure distribution around the injection hole is a function of the injection flow rate and determines the major directions in which the solute would start to flow from the injection point. For small injection flow rates, the solute follows the flow pattern that was established prior to injection. As the injection flow rate increases, however, the solute tends to flow radially from the injection point, and, in particular, may even flow away from the collection point.

As an example, we would like to show some detailed results of one of the generated fractures. The water flow paths with a negligible injection flow rate are shown in Figure 2. For this fracture, simulations were performed at three injection locations (n_x, n_y), given by (15,15), (11,11), and (8,8), respectively.

For injection at (15,15), the breakthrough curves show only one peak for the range of injection flow rates used in the simulations ($0.003Q$ to $0.03Q$). The tails of the breakthrough curves increase with increasing injection flow rates. This could be explained as follows. Original flow at the injection point is small, but the injection point is located close to a path with enough good connections to the collection hole. Thus, as flow rate increases, more and more solute feeds into this channel, giving rise to the longer tail.

The breakthrough curves for injection at (11,11) show one peak over the whole range of injection flow rates used (from $0.001Q$ to $0.03Q$). The fracture apertures around the injection point are large, and the flow rate in the injection point is also large. The patterns for the solute transport are then similar for all cases having different injection flow rates.

For injection at (8,8), the breakthrough curve for tracer concentration shows one peak for flow rates smaller than $0.003Q$. When the flow rate is increased beyond this value, a new peak starts to build up at a shorter residence time and the previous peak is reduced. For an injection flow rate of $0.03Q$, the peak at the short residence time is larger than the peak at the longer residence time. This variation of the relative sizes of the peaks is shown in Figure 3. The patterns of solute transport are shown in Figure 4. For an injection flow rate of $0.01Q$, new transport paths are created near the injection point, but the solute paths farther away are similar to those at lower flow rates. When the flow rate is increased even more, new paths are formed and new areas away from the injection point are involved in solute transport (Figure 4).

SUMMARY OF THE RESULTS

From the results of our many simulations, we distinguish the following causes of injection tracer tests:

• If injection occurs on a main flow channel in the fracture plane, the breakthrough curve would possess a single peak. This peak is almost independent of the injection flow rate.
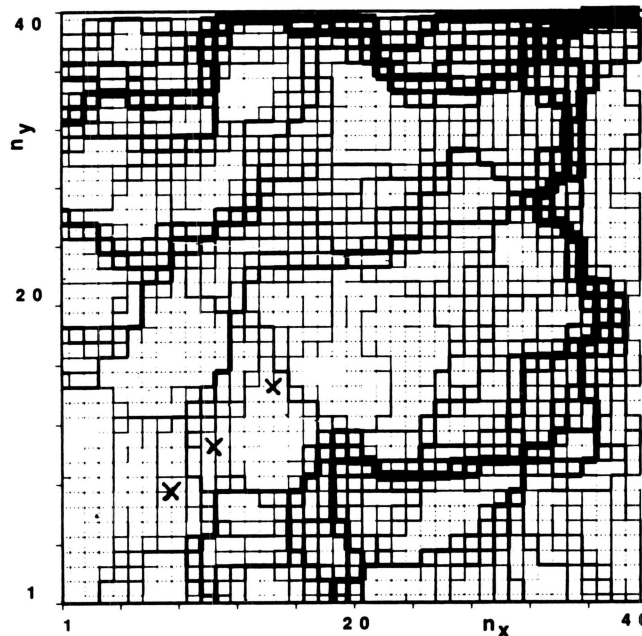

Figure 2. Flow paths in fracture 3 for a negligible injection flow rate. The injection points ("x") are (15,15), (11,11), and (8,8). [XBL 935-781]
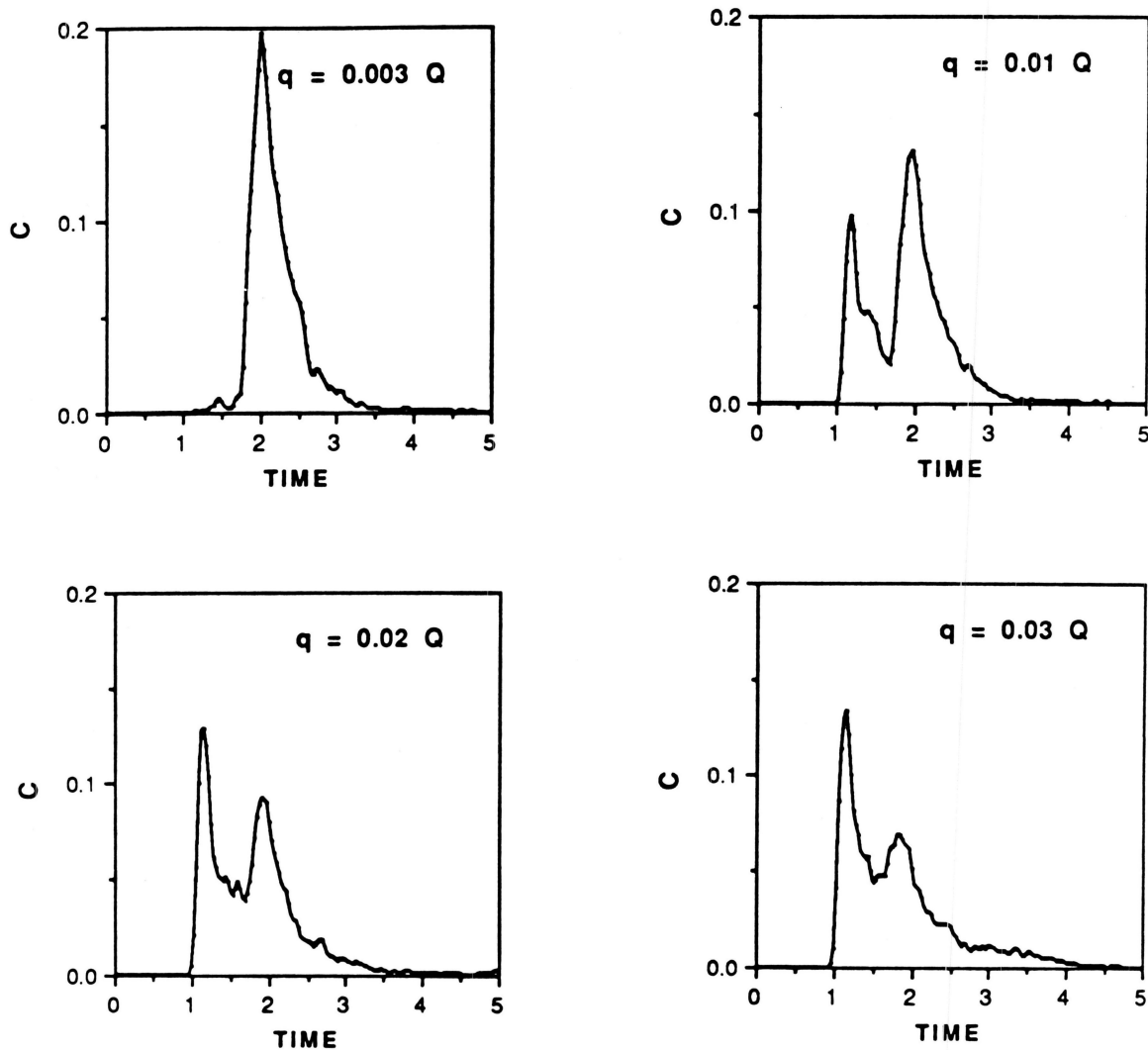
132

Figure 3. Breakthrough curves for fracture 3, for injection flow rates of $0.003Q$, $0.01Q$, $0.02Q$, and $0.03Q$. Injection at (8,8). [XBL 935-782]

- If injection does not occur on a main flow channel, multiple peaks may be observed.

- Dispersion depends on the number of possible paths near injection point.

In the case where injection does not occur on a main flow channel, we distinguish three possible alternative cases:

- A time shift of the first peak with a variation of the injection flow rate: the residence time decreases with an increase of the injection flow rate.

- When the injection flow rate is increased, the magnitude of the first peak decreases and the second peak builds up. Additional small peaks for long residence times may also emerge.

- Alternatively, when the injection flow rate is increased, the magnitude of the first peak increases.

The discussion and results given here may equally apply to tracer tests in a two-dimensional strongly heterogeneous medium. Although there are differences in permeability-porosity relationships between fractured and porous media, we expect that qualitatively the multiple-peak tracer transport behavior as discussed here should also be expected in such heterogeneous porous medium systems.
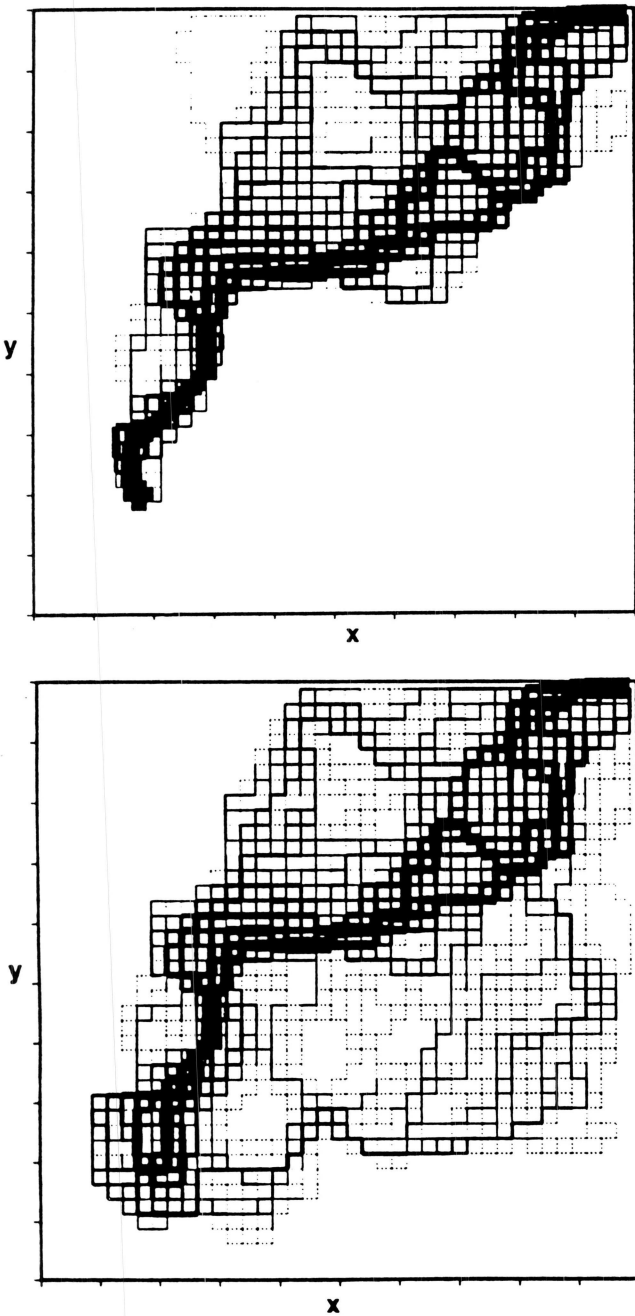
ACKNOWLEDGMENTS

Figure 4. Tracer paths in fracture 3 for an injection flow rate of $0.003Q$ and $0.03Q$. Injection at (8,8). [XBL 935-783]

REFERENCES

Abelin, H., Neretnieks, I., Tunbrant, S., Moreno, L., 1985. Final report of the migration in a single fracture, experimental results and evaluation. Stripa Project TR 85-03, Nuclear Fueled Safety Project, Stockholm, Sweden.

Hoehn, E., Frick, U., and Hadermann, J., 1989. A radionuclide migration experiment in fractured granitic rock. *In* Proceedings, International Symposium on Processes Governing the Movement and Fate of Contaminants in the Subsurface Environment, Stanford, California, July 24–26.

Moreno, L., Tsang, Y.W., Tsang, C.F., Hale, F.V., and Neretnieks, I., 1988. Flow and tracer transport in a single fracture: A stochastic model and its relation to some field observations. Water Resour. Res., v. 24, no. 12, p. 2033-2048 (LBL-25049).

Moreno, L., Tsang, C.F., Tsang, Y., and Neretnieks, I., 1990. Some anomalous features of flow and solute transport arising from fracture aperture variability. Water Resour. Res., v. 26, no. 10, p. 2377–2391.

Neretnieks, I., 1987. Channeling effects in flow and transport in fractured rocks—Some recent observations and models. Swedish Nuclear Power Inspectorate, Proceedings of GEOVAL-87, Stockholm, Sweden.

Robinson, P.C., 1984. Connectivity, flow and transport in network models of fractured media. Ph.D. Thesis, Oxford University, Oxford.

Schwartz, F.W., Smith, L., and Crowe, A.S., 1983. A stochastic analysis of macroscopic dispersion in fractured media. Water Resour. Res., v. 19, no. 5, p. 1253–1265.

Steffen, P., and Steiger, H., 1988. NAGRA Felslabor Grimsel, Migration, Traceruntersuchungen, Vorversuche 1–4, GEMAG (Aktiengesellschaft für Geologisch-Physikalische Messungen), Alberswil, Switzerland.

Tsang, Y.W., and Tsang, C.F., 1989. Flow channeling in a single fracture as a two-dimensional strongly heterogeneous permeable media. Water Resour. Res., v. 25, no. 9, p. 2076–2080 (LBL-26595).